Early Assessment Window for Predicting Breast Cancer Neoadjuvant Therapy Using Biomarkers, Ultrasound, and Diffuse Optical Tomography

Quing Zhu (zhu.q@wustl.edu)
Washington University in St Louis https://orcid.org/0000-0002-1837-2588
Foluso O Ademuyiwa
Washington University in Saint Louis
Catherine Young
Baylor Scott and White Central Texas
Catherine Appleton
Saint Luke's Hospital
Matthew F Covington
University of Utah Hospital
Cynthia Ma
Washington University in Saint Louis
Souzan Sanati
Cedars-Sinai Medical Center
Ian S Hagemann
Washington University in Saint Louis
Atahar Mostafa
Washington University in Saint Louis
K. M. Shihab Uddin
Washington University in Saint Louis
Isabella Grigsby
Washington University in Saint Louis
Ashley E Frith
Washington University in Saint Louis
Leonel Hernandez Aya
Washington University in Saint Louis
Steven P Poplack
Stanford University School of Medicine

Research article

Keywords: Predicting Neoadjuvant therapy, Personalized Medicine, Near Infrared imaging, Ultrasound

Posted Date: August 12th, 2020

DOI: https://doi.org/10.21203/rs.3.rs-54759/v1

Version of Record: A version of this preprint was published at Breast Cancer Research and Treatment on May 10th, 2021. See the published version at https://doi.org/10.1007/s10549-021-06239-y.

Abstract

Background:

Neoadjuvant Therapy (NAT) permits less aggressive breast and axillary surgery and better assessment of systemic response. Establishing accurate and early predictors of NAT response would help limit morbidity of ineffective regimens through modification of treatment regimens and thereby optimize clinical outcomes. The purpose of the study was to assess the utility of tumor biomarkers, ultrasound (US) and US-guided diffuse optical tomography (DOT) in early prediction of breast cancer response to NAT.

Methods

This prospective HIPAA compliant study was approved by the institutional review board. Forty one patients were imaged with US and US-guided DOT prior to NAT, at completion of the first three treatment cycles, and prior to definitive surgery from February 2017 to January 2020. Miller-Payne grading was used to assess pathologic response. Receiver operating characteristic curves (ROCs) were derived from logistic regression using independent variables, including: tumor biomarkers, US maximum diameter, percentage reduction of the diameter (%US), pretreatment maximum total hemoglobin concentration (HbT) and percentage reduction in HbT (%HbT) at different treatment time points. Resulting ROCs were compared using area under the curve (AUC). Statistical significance was tested using two-sided two-sample student t-test with $P<0.05$ considered statistically significant.

Results

Thirty-eight patients (mean age =47, range 24-71 years) successfully completed the study, including 15 HER2+ of which 11 were ER+; 12 ER+ or PR+/HER2-, and 11 triple negative. The combination of HER2 and ER biomarkers, %HbT at the end of cycle 1 (EOC1) and %US (EOC1) provided the best early prediction, AUC = 0.941 (95% CI: 0.869–1.0). Similarly an AUC of 0.910 (95% CI: 0.810–1.0) with %US (EOC1) and %HbT (EOC1) can be achieved independent of HER2 and ER status. The most accurate prediction, AUC = 0.974 (95% CI: 0.933–1.0), was achieved with %US at EOC1 and %HbT (EOC3) independent of biomarker status.

Conclusion

The combined use of tumor HER2 and ER status, US, and US-guided DOT may provide accurate prediction of NAT response as early as the completion of the first treatment cycle.

Clinical Trial Registration number: NCT02891681

Registration time: September 7, 2016

https://clinicaltrials.gov/ct2/show/NCT02891681

Introduction

Preoperative neoadjuvant therapy (NAT) for patients with locally advanced breast cancer downstages the tumor to facilitate breast conserving surgery, and allows in vivo assessment of therapeutic efficacy for tailored

treatment approaches. Pathological response to NAT predicts clinical outcome. An absence of residual invasive breast cancer cells, in the primary tumor bed and lymph nodes following NAT is strongly correlated with improved disease-free survival and overall survival (1). However, breast cancer is a heterogeneous disease; approximately 20–25% of breast cancers have amplification of the human epidermal growth factor receptor 2 (HER-2/neu), while 10–20% of breast cancers lack expression of estrogen receptor and progesterone receptor and HER2 gene amplification, known as triple-negative breast cancer (TNBC). Dual HER2 blockade in the neoadjuvant setting has been shown to increase the pCR rate in HER2 positive disease (2–4). Despite this, there is a significant percentage of HER2 + patients who do not achieve a pCR or near pCR (5). Those patients who have residual invasive breast cancer after HER2-targeted therapies have a worse prognosis (6). Moreover, to date, no FDA-approved targeted therapies are available for early-stage TNBC patients and refining TNBC breast cancers into molecular subtypes still is a significant challenge in predicting NAT (7). Thus, there is an unmet need for individual assessment before and during early NAC to guide treatment options by switching patients to other therapies to achieve optimal outcomes with reduced toxicity.

Many ongoing investigations are exploring imaging techniques to monitor response. The use of imaging is appealing because it is non-invasive and may provide a window of opportunity wherein ineffective treatment regimens could be altered. Conventional imaging methods include mammography, ultrasound (US), magnetic resonance imaging (MRI), and PET-CT. Mammography has low sensitivity in the evaluation of NAT response (8). US is moderately accurate (9–12) and has the additional benefits of easy access and low cost. MRI and PET-CT have both demonstrated high accuracy in predicting pCR (13–15). However, both MRI and PET-CT are potentially cost prohibitive given the need for serial imaging evaluation.

Optical tomography and spectroscopy using near infrared (NIR) diffused light has been explored as a novel tool to predict and monitor tumor vasculature response to NAT (16–26). The NIR technique utilizes intrinsic hemoglobin contrast, which is related to tumor angiogenesis. Recently studies have shown that pre-treatment total hemoglobin concentration (HbT) and changes in HbT measured at the early treatment cycles can predict treatment outcome (16–26). Furthermore, the Diffuse Optical Tomography (DOT) can be easily integrated with ultrasound systems for dual-modality imaging assessment of breast cancer response to NAT. This manuscript reports a three-year prospective study of a considerable patient population evaluated with US and US-guided DOT before, during, and after treatment completion in an attempt to identify the best and earliest predictors of pCR for HER2+, ER+/HER2- and triple negative breast cancer subtypes.

Materials And Methods

Patient

This prospective study was approved by the local institutional review board and was HIPAA compliant. Sixty female patients with newly diagnosed breast cancer presenting to medical oncology at Washington University School of Medicine from February 2017 to August 2019 for preoperative systemic therapy signed informed consent. Exclusion criteria included pregnancy, breastfeeding, prior history of breast cancer, prior history of chest wall radiation, prior history of breast reconstruction, reduction, or augmentation and bilateral breast cancers, biopsy less than 7 days of imaging. Fifteen patients were subsequently deemed ineligible including biopsy less than 7 days before imaging (n = 3), contralateral masses in mirror positions (n = 2), prior cancer

mastectomy of one breast (n = 2), prior breast reduction or radiation (n = 2), schedule restriction to participate the study (n = 6) and 4 withdrew (see Fig. 1). Of the remaining 41 patients, two developed metastases and did not complete the study and one had a contralateral abnormality preventing reference imaging. Data from these three patients were not included in the analysis. Thus 38 female patients (mean age = 47, range 24–71 years) constituted the study group and underwent US and US-guided DOT imaging of the index breast cancer prior to the initiation of NAT, at the end of the first three treatment cycles and before definitive surgery. Patients were treated with NAT regimens according to current clinical practice or based on therapeutic trial protocols.

Baseline imaging was performed an average of 28 days after diagnostic core needle biopsy (median = 26, range 7–56 days) and before the first treatment (median = 1 day, range 0–15 days). During treatment, imaging occurred before patient scheduled treatment (median = 0, range 0–5 days). The average interval between post-treatment imaging and definitive surgery was 25 days (median 20, range 1–163 days).

Us And Us-guided Dot Imaging

Ultrasound and US-guided DOT examinations were completed in a breast imaging clinic with 4 commercial US units and associated US probes of SL15-4 (Aixplorer™, SuperSonic Imagine Inc., Aix-en-Provence, FR) and a 4th generation DOT system. Standard US was performed by one of four dedicated breast imaging radiologists with an average of 12 years of breast US experience (range 2–24 years) at study initiation. The index tumor was imaged in orthogonal planes and the maximum diameter was recorded. Prior US examinations were referenced during the exam to ensure consistency of measurements. The percentage ratio %US, largest dimension of each post-treatment time point over the largest dimension pretreatment, was used to evaluate the fraction reduction from NAT. After completion of the breast US examination, the commercial US probe was inserted into the DOT probe. The breast radiologist then directed the engineer to the index tumor site and assisted in US-guided DOT acquisition as needed.

Details of the 4th generation DOT system used for this trial have been previously reported (27). Briefly, the US-guided DOT probe consists of the commercial US transducer located centrally, with source and detector light guides (optical fibers) distributed around the periphery. The foot print of the DOT probe is approximately 9 cm. Four source laser diodes of 730 nm, 785 nm, 808 nm and 830 nm optical wavelengths were sequentially switched to nine positions on the probe, while the reflected light was coupled by the light guides to 14 parallel detectors. The entire NIR data acquisition interval was less than 5 seconds. For each patient, US images and optical measurements were acquired simultaneously of both the index tumor site and subsequently a normal region within the corresponding quadrant of the contralateral breast (see insert of Fig. 3). Multiple datasets were acquired of the index tumor and contralateral reference site. The perturbation or scattered field caused by tumor, , between the measurements of the tumor site and the reference site was used for image reconstruction. The measurements from the normal contralateral breast were used for calculating the background optical absorption and reduced scattering coefficients which were used for computing weight matrix for image reconstruction.

The optical-imaging reconstruction algorithm has been described and validated (28). In brief, the reconstruction problem is formulated as :

$$Obj(X) = \min_X(\|U_{sc} - WX\|^2 + \frac{\lambda}{2}\|(X)\|^2)$$

where X is the unknown optical absorption distribution of the tissue that can be determined from the measured data U_{sc}, W and λ is a regularization parameter determined from the largest eigenvalue of

$WW^{\dagger}$.

A conjugate gradient optimization method is employed to solve the above inverse problem. Furthermore, the DOT reconstruction uses ultrasound lesion identification to segment the imaging volume into a region of interest (ROI) and background to improve the inversion. The ROI is two to three times larger in spatial dimensions than the tumor size (as measured by co-registered US) due to the low spatial resolution of diffused light. A tighter ROI in the depth dimension is set by using co-registered US. The pretreatment ROI is used for data processing of all time points, thereby minimizing the effect of treatment related changes in tumor size on the optical image reconstruction.

The optical absorption distribution at each wavelength was reconstructed, and the total hemoglobin concentration (HbT), oxygenated-hemoglobin (oxyHb) and deoxygenated-hemoglobin concentration (deoxyHb) maps were computed. An average maximum value of HbT, oxyHb, and deoxyHb was obtained from 5–10 quality optical images reconstructed from each of the multiple data sets acquired from the index tumor. Data with patient motion as evaluated by using two co-registered US images before and after each optical data set were excluded from averaging. To assess each patient's response, the HbT obtained before treatment was taken as the baseline and the percentage (%HbT) normalized to the baseline was used to quantitatively evaluate the remaining tumor vascular fraction during NAT.

Pathology Assessment

Pathology data were extracted from pathology reports and from re-examination of formalin-fixed, paraffin-embedded slides to complete missing data. One breast pathologist (SS, 10 years experience) evaluated cases from patients recruited between February 2017 to May 2019 and the second breast pathologist (ISH, 7 years experience) evaluated the rest. Response to NAC therapy in each surgical resection specimen was graded using Miller-Payne (MP) criteria (29), with comparison to initial core biopsy when necessary. There are five MP grades based on reduction in tumor cellularity: Grade 1—no change or minor alteration in individual malignant cells but no reduction in overall cellularity (no response, pNR). Grade 2—minor (up to 30%) loss of tumor cells but overall cellularity remains high; partial pathologic response (pPR). Grade 3—estimated 30–90% reduction in tumor cells (pPR). Grade 4—marked (> 90%) disappearance of tumor cells or near-complete pathologic response (pCR). Grade 5—no malignant cells are identifiable in sections from the tumor bed (pCR), although residual ductal carcinoma *in situ* (DCIS) may be present. The MD Anderson residual cancer burden (RCB) was calculated based on the primary tumor bed, overall cancer cellularity, in situ disease, number of positive lymph nodes and diameter of the largest lymph node metastasis (30). Since US and US-guided DOT were performed on the index tumor, the MP grading system was used to evaluate pathological response and RCB was used as a reference.

Invasive carcinoma within the pretreatment core biopsies was graded using the Nottingham histologic score (NS). Testing for estrogen receptor (ER), progesterone receptor (PR), and HER2/neu (c-erbB-2) expression was performed by immunohistochemistry by an FDA-approved method on formalin-fixed, paraffin-embedded pretreatment core biopsy tissue. The ER and PR were scored by Allred scoring system (31), where the total score ranges from 0–8 (scores > 3 are positive). HER2 was scored in accordance with 2018 ASCO/CAP guidelines. Cases with equivocal HER2 immunostaining were reflexed to fluorescence in situ hybridization (FISH).

Statistical Analysis

Generalized Logistic Regression (GLR) was used to relate treatment outcomes to individual predictor variables for ROC analysis. Each predictor was first correlated with the MP grade using Spearman's rho correlation coefficient to assess its predictive value. The t-test was used to evaluate the statistical significance and *P* values less than 0.05 were considered significant. For each pair of significant predictors, a correlation between the two predictors was evaluated using Spearman's rho correlation coefficient. The correlated predictors were not used together for ROC analysis. Minitab 19 software (Minitab, State College, PA) was used for statistical calculations. When comparing %HbT and %US at different treatment cycles, the Bonferroni-Holm correction was applied to obtain the corrected *P* value for the number of treatment cycles. The 95% confidence interval (CI) of each ROC was computed in R using the pROC package. To evaluate the significance of different ROCs with different sets of predictors, we used a function deltaAUC in R, which was specially designed to compare AUCs with overlapping predictors (32).

In Appendix A, we developed treatment prediction models using combined data from 38 patients reported in this study and 22 patients acquired in an earlier study with similar DOT system parameters, patient and treatment characteristics (19).

Results

Table 1 summarizes patient and tumor characteristics, NAT regimens and MP grading. The histologic type of 35 patients was invasive ductal carcinoma of no special type; one patient had invasive mucinous carcinoma, one patient had invasive lobular carcinoma and one patient had invasive mammary carcinoma with mixed ductal and lobular features. One of the 38 patients had multi-focal disease consisting of three adjacent distinct tumor masses with identical histology. For this patient, the largest of the three masses was used for data analysis. Fifteen patients were HER2+, 11 were triple-negative (TNBC), and 12 were ER+/HER2- (n = 10) or PR+/HER2- (n = 2). Eight patients had stage 3 disease, 27– stage 2, and 3– stage 1. For the three patients with stage 1 disease, two had HER2 + tumors, and one had high grade TNBC. Based upon MP grade, 5 patients had no response (pNR) (MP1), 11 patients had a partial response (pPR), including 3 with a minor response (MP2) and 8 with an intermediate response (MP3), while 3 had a near-complete response (MP4) and 19 had a complete response (pCR) (MP5).

Table 1
Clinicopathologic characteristics, biomarkers, initial (clinical) tumor staging, residual (post-neoadjuvant) staging, residual cancer burden, treatment regimens, and Miller-Payne grade

Subject #	Age	Histology type	Grade[1] score	Biological subtype	Tumor Stage	Residual Tumor (gross)/RCB index	Treatment Regimen	Miller-Payne grade
NIR005	40	IDC	Intermed (6)	ER + PR + HER2-	T2	2.1/2.796	ACT	3
NIR006	44	IDC	High (9)	ER-PR-HER2-	T2	0/0	ACT	5
NIR008	31	IDC	High (9)	ER + PR + HER2-	T2	0.8/2.73	ACT	3
NIR011	45	IDC	High (9)	ER-PR-HER-	T2	0/0	ACT	5
NIR014	38	IDC	Intermed (6)	ER + PR + HER2-	T2	2.5/3.19	ACT	2
NIR015	61	IDC	High (9)	ER-PR + HER2-	T2	2.4/2.368	ACT	1
NIR021	59	IDC	High (8)	ER-PR-HER-	T1	0/0	ACT	5
NIR023	65	IDC	High (9)	ER-PR-HER2-	T2	0.3/1.333	ACT	3
NIR025	59	IDC	High (9)	ER-PR-HER2-	T3	0/0	ACT	5
NIR026	45	IDC	High (9)	ER + PR + HER2-	T2	0.7/1.355	ACT	4
NIR027	41	IDC	High (9)	ER + PR-HER-	T2	3.1/3.52	ACT	1
NIR034	35	IDC	High (8)	ER + PR + HER2 -	T2	1.2/2.953	ACT	2
NIR038	44	IDC	Intermed (5)	ER + PR + HER2-	T3	2.0/4.024	ACT	3
NIR041	48	ILC	Intermed (5)	ER + PR + HER-	T3	4.1/4.251	ACT	1
NIR001	62	IDC	High (8)	ER + PR + HER2+	T2	0/0	TCHP	5
NIR003	48	IMC	Intermed(4)	ER + PR + HER2+	T2	2.9/1.642	TCHP	1
NIR007	42	IDC	High (9)	ER- PR-HER2+	T3	0/0	TCHP	5

Subject #	Age	Histology type	Grade[1] score	Biological subtype	Tumor Stage	Residual Tumor (gross)/RCB index	Treatment Regimen	Miller-Payne grade
NIR010	39	IDC	High (9)	ER + PR- HER2+	T2	0/0	TCHP	5
NIR018	44	IDC	High (7)	ER-PR- HER2+	T2	0/0	TCHP	5
NIR019	37	IDC	High (9)	ER + PR + Her2+	T2	0/0	TCHP	5
NIR022	30	IDC	High (9)	ER-PR- HER2+	T2	0/0	TCHP	5
NIR029	52	IDC	High (8)	ER + PR- HER2+	T2	0/0	TCHP	5
NIR032	38	IDC	Intermed(6)	ER + PR- HER2+	T3	0/0	TCHP	5
NIR035	50	IDC	High (7)	ER-PR- HER2+	T1	0/0	TCHP	5
NIR040	34	IDC	High (7)	ER + PR + HER+	T2	0.2/1.277	TCHP	4
NIR004	50	IDC	High (9)	ER-PR- HER2-	T3	0/0	CarboT	5
NIR009	38	IDC	High (8)	ER-PR + HER- PR + HER2-	T2	0/0	CarboT	5
NIR016	53	IDC	High (9)	ER + [2]PR- HER2-	T2	0/0	CarboT	5
NIR020	48	IDC	High (7)	ER-PR- HER2-	T2	0.15/1.899	CarboT	3
NIR030	71	IDC	High(9)	ER-PR- HER2-	T2	0.9/2.045	CarboT	2
NIR031	24	IDC	High (9)	ER-PR- HER2-	T3	0/0	CarboT - AC	5
NIR012	49	IDC	High (9)	ER- PR- HER2-	T2	0/0	ACP	5
NIR028	39	IDC	High (8)	ER-PR- HER2-	T2	2.5/3.82	ACP	3
NIR013	52	IDC	High (9)	ER + PR- HER2+	T3	1.3/1.59	PLT	3

Subject #	Age	Histology type	Grade[1] score	Biological subtype	Tumor Stage	Residual Tumor (gross)/RCB index	Treatment Regimen	Miller-Payne grade
NIR033	56	IDC/ILC	High (9)	ER + PR- HER2+	T2	1.1/1.561	PLT	3
NIR036	57	IDC	High (8)	ER + PR + HER2+	T2	0.1/0.598	PLT	4
NIR037	43	IDC	High (7)	ER + PR + HER2+	T1	0/0	PLT	5
NIR039	66	IDC	Intermed (5)	ER + PR + HER2–	T2	1.5/3.222	Anastrazole	1
1. Nottingham Grade: 1–3 low, 4–6 intermediate, 7–9 high								
2. Initial receptor report from outside hospital was TNBC and corrected later as ER+.								
IDC, invasive ductal carcinoma								
IMC, invasive mucinous carcinoma								
ILC, invasive lobular carcinoma								
TCHP: Docetaxel, carboplatin, trastuzumab, and pertuzumab								
ACT: AC (Doxorubicin hydrochloride and cyclophosphamide) every two weeks followed by weekly paclitaxel (Taxol) for 12 weeks								
CarboT: Carboplatin (Paraplatin) and Docetaxel (Taxotere)								
ClinicalTrials.gov Identifier: NCT02124902								
ACP: Atezolizumab Carboplatin Paclitaxel								
ClinicalTrials.gov Identifier: NCT02883062								
PLT: Palbociclib Letrozole Trastuzumab								
ClinicalTrials.gov Identifier: NCT02907918								
CarboT-AC: Carboplatin and Docetaxel for four cycles followed by Doxorubicin (adriamycin) / Cyclophosphamide								

Tumor characteristics, US measurements and optical parameters were correlated to pathologic outcomes, i.e., non- or incomplete response (MP1–3) vs. near-complete or complete response (MP4–5) using the Spearman's rho correlation. HER2 + status was significantly associated with MP4–5 (P = 0.039), and ER+/HER2– status was significantly associated with MP1–3 (P = 0.036), while Nottingham grade and triple-negative status were not (P = 0.115, P = 0.138). Pretreatment maximum tumor size measured by US corresponded to an incomplete response (P = 0.011). MP1–3 had a baseline maximum of 34.4 mm 12.8 mm, vs. 26.9 mm 10.9 mm for MP4–5, but the difference between the two responder groups was not statistically significant (P = 0.066). Reduction in tumor size compared to pretreatment baseline (%US) at the end of each of the first three cycles was

associated with a pCR (EOC 1, P = 0.005, EOC 2, P = 0.045, EOC 3, P = 0.013), especially at EOC1. Post-treatment %US was not associated with a pCR (P = 0.134), however, post-treatment tumor size was associated a pCR (P = 0.012). Pretreatment HbT correlated with a complete response (P = 0.028), while oxyHb and deoxyHb were not (P = 0.091, P = 0.132). Reduction in HbT (%HbT) showed the strongest correlation with a pCR at the end of each of the first three cycles (P = 0.001, P < 0.001, P < 0.001). Post-treatment %HbT also showed a strong correlation with a pCR (P = 0.007).

Figure 2 demonstrates the HbT, reduction in HbT, %HbT, and reduction in tumor size, %US, over the first three treatment cycles. Bonferroni-Holm correction was applied to adjust for multiple comparisons of %HbT and %US over treatment cycles. There was a difference in pretreatment mean maximum HbT between MP1–3 vs. MP4–5. MP4–5 tumors had a pretreatment HbT of 85.9 M 20.0 [standard deviation], vs. 71.3M 19.1 for MP1–3 (P = 0.029) (Fig. 2A). However, there was no difference at EOC1 or EOC2 because the mean HbT level decreased at a faster rate in complete responders. At EOC3 complete responders had a significantly lower HbT. The faster rate of reduction is best visualized in Fig. 2B. MP4–5 tumors decreased rapidly to 78% (of baseline)18.9, 64.2%18.5, 48.2%13.8 at EOC1, EOC2 and EOC3, respectively, whereas MP1–3 tumors changed minimally to 97.3%22.6 (EOC1), 88.7%22.9 (EOC2), and 89.0%26.4(EOC3). The differences between the two groups were increasingly significant as treatment progressed through the first three cycles; Pc = 0.012 (EOC1), Pc = 0.008 (EOC2) and Pc < 0.001 (EOC3), respectively.

The %US measurements showed a similar trend. The reduction in diameter was significant with reduction rate of 74.8%17.8, 61.8% 28.3, 52.4% 29.4 in MP4-5 tumors and 96.5% 17.8, 82.4%23.7 and 74.7% 23.5 in MP1-3 tumors, respectively (Fig. 2C). The differences between the two groups were significant with Pc = 0.003 (EOC1), Pc = 0.028 (EOC2), Pc = 0.040 (EOC3), respectively.

Examples of a treatment responder and a non-responder are shown in Figs. 3 and 4.

We performed ROC analyses using logistic regression to identify the best early predictors of response (MP4-5) at different treatment time points, EOC1-3. Incremental AUCs are tabulated (Table 2) with and without predictive biomarker status of ER and HER2, and subsets ROCs shown graphically in Fig. 5. As noted above only HER2 and ER status were shown to predict treatment response (AUC = 0.773, 95% CI: 0.629–0.917). When added to ER and HER2 status, %US at EOC1 noticeably improves the AUC (AUC = 0.883, 95% CI: 0.768–0.997). Similarly, the addition of %HbT to biomarker status substantially increases the AUC. While each parameter is independently helpful, the combination of %US and %HbT is most effective in enhancing the prediction. The combination of predictive biomarkers, %US and %HbT at EOC1 provides the best prediction of response at the earliest time point, AUC = 0.941 (95% CI: 0.869–1.0), which is significant when compared with biomarkers and %US at EOC1 (P < 0.001). The greatest AUC of any time during early treatment (AUC = 0.974, 95% CI: 0.932–1.0) is achieved through the combination of predictive biomarkers, %US (EOC1) and %HbT (EOC3), which is also significant when compared with biomarkers and %US at EOC1 (P < 0.001). Even in the absence of ER and HER2 status, the identical maximum AUC is achieved (AUC = 0.974, 95% CI: 0.933-1.0) using %US (EOC1) and %HbT (EOC3), with only slight diminution at the earliest time point, i.e. %US (EOC1) and %HbT (EOC1), AUC = 0.910 (95% CI: 0.810–1.0). The AUC improvements of adding %HbT (EOC1) and %HbT (EOC3) to %US (EOC1) is statistically significant (P < 0.001). Note that Miller-Payne grade and RCB are highly correlated, Spearman's rho = 0.941 (P < 0.001). To improve the robustness of the prediction we have combined data from the 38

patients in this study with earlier data of a smaller patient population of 22 patients. Similar results were obtained (details in Appendix A).

Table 2

Logistic regression models based on tumor subtypes (HER2, ER) and TNBC, US measurements, and hemoglobin parameters, AUC. Data were from this study of total 38 patients.

ROC Analysis including HER2 and ER Biomarker status			
Biomarkers, HbT and US measured before NAT	Biomarkers, %US measured at EOCs 1–3	Biomarkers, HbT, %HbT measured at EOCs 1–3	Biomarkers, %HbT and %US measured at EOCs 1–3
• HER2, ER AUC = 0.773 95% CI: 0.629–0.917 • HER2, ER, HbT AUC = 0.804 95% CI: 0.659–0.949	• HER2, ER, %US_EOC1 AUC = 0.883 95% CI: 0.768–0.997 • HER2, ER, %US_EOC2 AUC = 0.771 95% CI: 0.608–0.935 • HER2, ER, %US_EOC3 • AUC = 0.842 95% CI: 0.710–0.975	• HER2, ER, HbT, %HbT_EOC1 AUC = 0.903 95% CI: 0.808–0.998 • HER2, ER, HbT, %HbT_EOC2 AUC = 0.911 95% CI: 0.811–1.0 • HER2, ER, HbT, %HbT_EOC3 AUC = 0.968 95% CI:0.918–1.0	**• HER2, ER,%HbT_EOC1,%US_EOC1** **• AUC = 0.941** **95% CI: 0.869–1.0** • HER2, ER, %HbT_EOC2, %US_EOC2 AUC = 0.900 95% CI: 0.797–1.0 • HER2, ER, %HbT_EOC3, %US_EOC3 AUC = 0.968 95% CI: 0.918–1.0 **• HER2, ER, %HbT_EOC3,%US_EOC1** **AUC = 0.974** **95% CI: 0.932–1.0**
ROC Analysis using Imaging Parameters only			
Biomarkers, HbT and US measured before NAC	%US measured at EOCs 1–3	%HbT measured EOCs 1–3	%HbT and %US measured at EOCs 1–3

ROC Analysis including HER2 and ER Biomarker status			
• TNBC AUC = 0.557 95% CI: 0.407–0.707 • US AUC = 0.671 95% CI: 0.492–0.849 • HbT AUC = 0.707 95% CI:0.540–0.8744	• %US_EOC1 AUC = 0.828 95% CI: 0.685–0.971 • %US_EOC2 AUC = 0.679 95% CI: 0.489–0.869 • %US_EOC3 AUC = 0.723 95% CI: 0.547–0.898	• HbT, %HbT_EOC1 AUC = 0.825 95% CI: 0.684–0.966 • HbT, %HbT_EOC2 AUC = 0.839 95% CI: 0.706–0.973 • HbT, %HbT_EOC3 AUC = 0.944 95% CI: 0.870–1.0	**• HbT, %HbT_EOC1, %US_EOC1** **AUC = 0.910** 95% CI: 0.810–1.0 • %HbT_EOC2, %US_EOC2 AUC = 0.889 95% CI: 0.774–0.993 • %HbT_EOC3%US_EOC3 AUC = 0.944 95% CI: 0.870–1.0 **• %HbT_EOC3%, US_EOC1** **AUC = 0.974** **95% CI: 0.933–1.0**

Discussion

In current clinical practice, clinical breast examination, mammography, US, MRI, and PET-CT have been used to evaluate response in patients receiving NAC. In a comparative study of imaging modalities in 43 patients, Shin and colleagues showed increasing correlation with pathologic tumor size, with intra-class correlation coefficients of 0.65 for clinical breast exam, 0.69 for mammography, 0.78 for US and 0.97 for MRI (33). In a recent meta-analysis of 969 patients from 18 studies, MRI had a summary ROC (sROC) AUC of 0.89 (13). When comparing PET-CT to MRI in a meta-analysis of 13 studies with 575 patients, MRI was more accurate, summary ROC (sROC) AUC: 0.88 vs. 0.84 (34). In contrast, in a meta-analysis of 10 studies, PET-CT outperformed MRI during NAC treatment (15). Mammography and/or breast MRI are recommended by NCCN (35) and CT, MRI, FDG PET are endorsed by RECIST 1.1 (36). US has not been recommended for monitoring disease status in clinical trials due to its perceived subjectivity and operator dependence (37).

However, because of its low cost and accessibility, US has been utilized and evaluated in several studies (9–12). In the GepharTrio trial of 2090 patients bidimensional US measurements at EOC2 were used to classify response and randomize patients to treatment with 6 vs 8 cycles of NAC (11). Candelaria and colleagues evaluated mid-treatment breast US in 159 patients and showed association of percentage change in tumor US measurements with RCB in TNBC and hormone receptor (HR) + and HER2− tumors but not in HR− and HER2 + tumors (10). Marinovich and colleagues applied RECIST 1.1 and WHO 1D and 2D measurement criteria in 832 patients who underwent US at EOC2 and demonstrated an average increase in AUCs of 2% and 3% to 0.79 and 0.80 respectively, with the addition of US to patient characteristics including biomarkers (9). In this study, we found that the fractional change of US maximum diameter (%US), measured at EOC1 (AUC = 0.83) was more predictive than EOC2 (AUC = 0.68). We further showed a substantial 11% increase, AUC = 0.77 to 0.88 at EOC1,

in patients with known ER + or HER2 + disease. We believe that early US measurements at EOC1 can substantially avoid measurement uncertainty caused by treatment induced inflammatory and fibrotic changes in the tumor bed.

Recently studies of shear wave elastography (SWE) have shown that increased extracellular matrix stiffness is associated with tumor progression and NCT resistance (38–39). SWE measures significant differences in tumor elasticity changes in pCR vs. non-pCR cases and AUCs of 0.613 (baseline), 0.745 (EOC1), 0.685 (EOC2) have reported in a recent clinical trial (40). This tread is similar to our study using gray scale US.

Diffuse optical tomography and diffuse optical spectroscopy exploit changes in tumor vascularity and metabolism and have demonstrated the potential for early prediction of breast cancer pathological response (18–26). Studies have shown accurate predictions in the neoadjuvant setting by utilizing pretreatment hemoglobin levels and changes in hemoglobin early in the course of treatment (19,21–26), or by monitoring changes of blood oxygen saturation sO2 at day 1 of dose dense treatment (18) or day 10 during early treatment (20). In the recent ACRIN 6691 trial evaluating 36 patients, the authors derived a tissue optical index (TOI), a product of deoxygenated Hb and water concentration over lipid, and reported that the mid-treatment TOI can predict pCR with AUC 0.6 to 0.83 (19). Gunther and colleagues developed a dynamic diffuse optical tomography system that could distinguish between response groups. An ROC analysis showed that this method could identify patients with a pCR two weeks into the treatment with AUC = 0.85 (17). In an earlier investigation using data from two studies with limited patients treated with new dual HER2 blockade regiment (19), Zhu and colleagues developed prediction models identifying HER2 status and HbT as the best pretreatment predictors of pCR (AUC = 0.88). The pretreatment predictors “ER status and HbT”, and “TNBC and HbT” predicted response with moderate AUC accuracies of 0.69 and 0.72, which are similar to the single predictor HbT (AUC = 0.75). With known HER2 positivity, the best window to accurately predict response was at the completion of the first and second cycles of NAT (AUC = 0.96, AUC = 0.97). For ER+/HER2- or TNBC subtype, the best window was at the completion of the first cycle of NAT and the best predictors were HbT and %HbT (AUC = 0.95).

In this new cohort of 38 patients, “HER2, ER and pretreatment HbT” has shown good prediction, AUC = 0.80 and HbT alone has shown moderate prediction AUC = 0.71. However, fractional reduction of HbT (%HbT) is a much more powerful predictor of response as is fractional reduction of maximum diameter measured with US (%US) in the first three cycles. In particular, combining tumor HER2 and ER status, %US EOC1 and %HbT at EOC1 provided the best early indicator of treatment response, AUC = 0.941, and remained powerful even without biomarker data, i.e. AUC = 0.910. As expected from log cell-kill kinetics of cytotoxic drugs, a given dose kills a constant proportion of a tumor cell population rather than constant number of cells (41). Therefore, for chemo-sensitive tumors, there are more total cells killed in the first cycle of treatment and more tumor neovasculature damage which may cause a significant decrease in tumor hemoglobin measured by the DOT system and size reduction measured by US. Overall, the highest accuracy, AUC = 0.974, was achieved with the combination of %US EOC1 and %HbT at EOC3 irrespective of biomarker status. To our knowledge, these AUC values are among the highest reported results using NAT regimens in current clinical practice.

From an exam delivery perspective, the combination of US and US-guided DOT provides important potential benefits for assessing NAT response compared to PET-CT and MRI. In the system used in this study, a

commercial US probe was used for US measurements and then placed within the fiber-optic array to guide DOT. Furthermore, in future iterations US could be completely integrated into a hybrid US – DOT system. The combined exam has no ionizing radiation, has low intrinsic cost, is easily adaptable to current equipment, and could be made widely available and portable. In contrast PET-CT and MRI are high cost and have limited access. Additionally, MRI has associated medical risks and contraindications. Disadvantages to US/US-guided DOT include: US-guided DOT imaging is not real-time and reconstruction currently takes a minimum of 20 to 30 minutes in computation time. US-guided DOT is not suitable for imaging tumors in the dark nipple-areolar complex, and requires a sonographically visible index tumor and normal contralateral reference tissue. US-guided DOT data acquisition requires training of operators to match the location of the lesion side and the contralateral reference side for differential measurements and can be performed by radiologists or US technologists. Dark skin absorbs more light than white skin, however, the DOT system has adequate source power to acquire measurements with good signal to noise ratio for a range of skin colors.

Our study has a number of limitations. This is a single institution experience and the imaging procedure was performed (US) and supervised (US-guided DOT) by dedicated breast imaging radiologists, which may affect the generalizability of results. The treatment regimens were based on current practice at a research institution and were not limited to a single regimen. The choice of systemic therapies for breast cancer patients are based on multiple factors, including tumor biology, stage, patient characteristics and wishes, clinical trial availability. The study population was not large (n = 38) and to develop prediction models, we included data from 22 patients from an earlier study with similar but not identical study criteria (19). While attempts were made to image the index tumor in the same orthogonal scan planes, i.e., radial-antiradial or transverse-sagittal, in order to optimize tumor conspicuity during treatment this was not always possible.

We chose our comparison groups as pCR and near pCR as “responders”, (Miller-Payne grades 4–5) versus “non-responders” (Miller-Payne grades 1–3), because the MP grading system is used to evaluate index tumor while residual cancer burden (RCB) additionally incorporates DCIS and lymph node status, which are not assessed by our DOT procedure. In our study Miller-Payne grade and RCB were highly correlated. Symmans et al. using the Residual Cancer Burden (RCB) system and another separate dataset for evaluating tumor response after neoadjuvant chemotherapy also found that pCR and near-pCR had very similar survivorship curves after surgery (30). Given that Ogston et al. originally reported that Miller-Payne grades 4 and 5 tended to track together with regard to 5 year disease free survive after neoadjuvant chemotherapy (29), we felt justified in considering MP 4 and MP 5 collectively as the responder group.

Only one patient was treated with an antiestrogen regimen, i.e. anastazole, in our study cohort. Due to the limited sample size, we have grouped this patient with the rest of the patients and used pCR as surrogate endpoint. However, pCR is uncommon in neoadjuvant endocrine treatment and a poor surrogate for disease free survival. Future studies assessing response to neoadjuvant endocrine therapy will likely rely on change in the proliferation marker Ki67 and the preoperative endocrine prognostic index (PEPI), a composite score of post-treatment ER, Ki67, tumor size and axillary nodal status, as a surrogate for endocrine sensitivity. Higher Ki67 and PEPI scores have shown to correlate with an increased risk of relapse (42).

Our study has substantial implications for the combined use of tumor subtypes, conventional US and near-infrared-measured tumor hemoglobin content in accurately predicting pathological response as soon as one

treatment cycle is completed. A recently phase 3, open-label trial involving patients with HER2-positive early breast cancer who were found to have residual invasive disease has shown that adjuvant trastuzumab emtansine (T-DM1) for 14 cycles reduced the risk of recurrence of invasive breast cancer or death by 50% as compared with trastuzumab alone (6). Another trial of 910 HER2– residual invasive breast cancer patients after neoadjuvant chemotherapy showed that adjuvant capecitabine was safe and effective in prolonging disease-free survival and overall survival (43). If the residual disease could be accurately estimated earlier in the NCT, patients with an unsatisfactory response could be switched to investigational therapies or even definitive surgery as soon as cycle 1 is completed, allowing for personalized treatment. This ability will gain value as our armamentarium of interventions increases and responses can more effectively tailor the therapeutic agents selected.

Conclusion

In conclusion, our results suggest that the combination of HER2 and ER status, %HbT at the end of cycle 1 (EOC1) and %US (EOC1) accurately predict NAT (AUC = 0.941), and %HbT (EOC1) and %US (EOC1) predict NAT (AUC = 0.910) regardless of HER2 and ER status. A greater prediction accuracy can be achieved with AUC of 0.974 regardless of biomarkers when the treatment window is extended to EOC3. Early assessment of response to NAT for breast cancer allows personalized treatment. The synergistic use of US and US-guided DOT may provide a safe, available, low cost strategy to accurately predict neoadjuvant treatment outcomes early in the course of therapy.

Abbreviations

NIR: Near Infrared; pCR: pathological complete response; ROI; region of interest; ER: estrogen receptor; PR: progesterone receptor; HER2: human epidermal growth factor receptor 2; NAT: neoadjuvant therapy; TNBC: triple-negative breast cancer; HbT: total hemoglobin; ROC: receiver operating characteristic curve; AUC: area under receiving operating characteristic curve;

Declarations

Acknowledgements

The authors appreciate the help of Clinical Trial Office of the Oncology Department of Washington University School of Medicine for patient consenting and scheduling.

Funding

The authors gratefully acknowledge the funding support of this project from the National Institutes of Health (R01EB002136, R01 CA228047). SPP acknowledges funding support from the Foundation for Barnes Jewish Hospital Ronald and Hanna Evens Endowed Chair in Women's Health.

Availability of data and material

The datasets used and/or analysed during the current study are available from the corresponding author on reasonable request.

Authors' contributions

QZ: designed and conducted all aspects of the ultrasound-guided optical tomography data acquisition, image reconstruction and data analysis and contributed to the manuscript preparation and literature review. SPP: designed and conducted patient imaging studies, data analysis, and contributed to the manuscript preparation and literature review. FOA and CM: coordinated and recruited patients to the study, and contributed to the manuscript review and literature review. CY, CA, MFC: contributed to the imaging studies, imaging interpretations, and manuscript review. SS and ISH: contributed to the pathological data evaluations, interpretations, manuscript review. AM and K.M.S.U: contributed to the development of optical tomography system hardware and software as well as imaging algorithm. IG: coordinated, consented all study patients, and data analysis. AEF and LFH: contributed to patient recruitments. All authors read and approved the final manuscript.

Drs. Catherine Young, Catherine Appleton, Matthew F. Covington, were faculty members of Radiology Department of Washington University in St Louis from the beginning of the study to July 2019. Dr. Steven Poplack was a faculty member of Radiology Department of Washington University in St Louis from the beginning of the study to June 2020.

Ethics approval and consent to participate

The study protocol was approved by institutional review board of Washington University School of Medicine in St Louis, and was HIPAA compliant. Written informed consent was obtained from all patients.

Consent for publication

All authors have read the manuscript and agreed with the submission.

Competing interests

QZ is the inventor of the patents related to ultrasound-guided near-infrared tomography technologies and patents owned by the University of Connecticut and/or Washington University in St Louis .

The authors declare that they have no competing interests.

References

1. Cortazar P, Zhang L, Untch M, Mehta K, Costantino JP, Wolmark N, Bonnefoi H, Cameron D, Gianni L, Valagussa P, Swain SM, Prowell T, Loibl S, Wickerham DL, Bogaerts J, Baselga J, Perou C, Blumenthal G, Blohmer J, Mamounas EP, Bergh J, Semiglazov V, Justice R, Eidtmann H, Paik S, Piccart M, Sridhara R,

Fasching PA, Slaets L, Tang S, Gerber B, Geyer CE Jr, Pazdur R, Ditsch N, Rastogi P, Eiermann W, von Minckwitz G.
Pathological complete response and long-term clinical benefit in breast cancer: the CTNeoBC pooled analysis. Lancet. 2014 Jul 12;384(9938):164-72. doi: 10.1016/S0140-6736(13)62422-8. Epub 2014 Feb 14.

2. Gianni L, Pienkowski T, Im YH, et al: Efficacy and safety of neoadjuvant pertuzumab and trastuzumab in women with locally advanced, inflammatory, or early HER2-positive breast cancer (NeoSphere): a randomised multicentre, open-label, phase 2 trial. Lancet Oncol 13:25-32, 2012
3. Hurvitz SA, Martin M, Symmans WF, Jung KH, Huang CS, Thompson AM, Harbeck N, Valero V, Stroyakovskiy D, Wildiers H, Campone M, Boileau JF, Beckmann MW, Afenjar K, Fresco R, Helms HJ, Xu J, Lin YG, Sparano J, Slamon D
Neoadjuvant trastuzumab, pertuzumab, and chemotherapy versus trastuzumab emtansine plus pertuzumab in patients with HER2-positive breast cancer (KRISTINE): a randomised, open-label, multicentre, phase 3 trial.
Lancet Oncol. 2018 Jan;19(1):115-126. doi: 10.1016/S1470-2045(17)30716-7. Epub 2017 Nov 23.
4. Schneeweiss A, Chia S, Hickish T, et al: Pertuzumab plus trastuzumab in combination with standard neoadjuvant anthracycline-containing and anthracycline-free chemotherapy regimens in patients with HER2-positive early breast cancer: a randomized phase II cardiac safety study (TRYPHAENA). Ann Oncol 24:2278-84, 2013
5. Krystel-Whittemore M, Xu J, Brogi E, Ventura K, Patil S, Ross DS, Dang C, Robson M, Norton L, Morrow M, Wen HY.
Pathologic complete response rate according to HER2 detection methods in HER2-positive breast cancer treated with neoadjuvant systemic therapy.10.1007/s10549-019-05295-9. Epub 2019 May 29.
6. von Minckwitz G, Huang CS, Mano MS, Loibl S, Mamounas EP, Untch M, Wolmark N, Rastogi P, Schneeweiss A, Redondo A, Fischer HH, Jacot W, Conlin AK, Arce-Salinas C, Wapnir IL, Jackisch C, DiGiovanna MP, Fasching PA, Crown JP, Wülfing P, Shao Z, Rota Caremoli E, Wu H, Lam LH, Tesarowski D, Smitt M, Douthwaite H, Singel SM, Geyer CE Jr; KATHERINE Investigators.
Trastuzumab Emtansine for Residual Invasive HER2-Positive Breast Cancer. N Engl J Med. 2019 Feb 14;380(7):617-628. doi: 10.1056/NEJMoa1814017. Epub 2018 Dec 5.
7. Lehmann BD, Jovanović B, Chen X, Estrada MV, Johnson KN, Shyr Y, Moses HL, Sanders ME, Pietenpol JA.
Refinement of Triple-Negative Breast Cancer Molecular Subtypes: Implications for Neoadjuvant Chemotherapy Selection.
PLoS One. 2016 Jun 16;11(6):e0157368. doi: 10.1371/journal.pone.0157368. eCollection 2016.
8. Accuracy of ultrasonography and mammography in predicting pathologic response after neoadjuvant chemotherapy for breast cancer.
Keune JD, Jeffe DB, Schootman M, Hoffman A, Gillanders WE, Aft RL. Am J Surg. 2010 Apr;199(4):477-84. doi: 10.1016/j.amjsurg.2009.03.012.
9. Marinovich ML, Houssami N, Macaskill P, von Minckwitz G, Blohmer JU, Irwig L.
Accuracy of ultrasound for predicting pathologic response during neoadjuvant therapy for breast cancer. Int J Cancer. 2015 Jun 1;136(11):2730-7. doi: 10.1002/ijc.29323. Epub 2014 Nov 25.

10. Candelaria RP, Bassett RL, Symmans WF, Ramineni M, Moulder SL, Kuerer HM, Thompson AM, Yang WT
Performance of Mid-Treatment Breast Ultrasound and Axillary Ultrasound in Predicting Response to Neoadjuvant Chemotherapy by Breast Cancer Subtype.
The Oncologist 2017; 22:394-401
11. von Minckwitz G1, Kümmel S, Vogel P, Hanusch C, Eidtmann H, Hilfrich J, Gerber B, Huober J, Costa SD, Jackisch C, Loibl S, Mehta K, Kaufmann M; German Breast Group.
Intensified neoadjuvant chemotherapy in early-responding breast cancer: phase III randomized GeparTrio study. J Natl Cancer Inst. 2008 Apr 16; 100: 552-562
12. Baumgartner A, Tausch C, Hosch S, Papassotiropoulos B, Varga Z, Rageth C, Baege A.
Ultrasound-based prediction of pathologic response to neoadjuvant chemotherapy in breast cancer patients.
Breast. 2018 Jun;39:19-23. doi: 10.1016/j.breast.2018.02.028. Epub 2018 Mar 7.
13. Magnetic Resonance Imaging Combined With Second-look Ultrasonography in Predicting Pathologic Complete Response After Neoadjuvant Chemotherapy in Primary Breast Cancer Patients.
Hayashi N, Tsunoda H, Namura M, Ochi T, Suzuki K, Yamauchi H, Nakamura S.
Clin Breast Cancer. 2019 Feb;19(1):71-77. doi: 10.1016/j.clbc.2018.08.004. Epub 2018 Aug 24.
14. Paydary K, Seraj SM, Zadeh MZ, Emamzadehfard S, Shamchi SP, Gholami S, Werner TJ, Alavi A. The Evolving Role of FDG-PET/CT in the Diagnosis, Staging, and Treatment of Breast Cancer.
Mol Imaging Biol. 2019 Feb;21(1):1-10. doi: 10.1007/s11307-018-1181-3.
15. Sheikhbahaei S, Trahan TJ, Xiao J, Taghipour M, Mena E, Connolly RM, Subramaniam RM FDG-PET/CT and MRI for Evaluation of Pathologic Response to Neoadjuvant Chemotherapy in Patients With Breast Cancer: A Meta-Analysis of Diagnostic Accuracy Studies.
Oncologist. 2016 Aug;21(8):931-9. doi: 10.1634/theoncologist.2015-0353. Epub 2016 Jul 8.
16. Tromberg BJ, Zhang Z, Leproux A, O'Sullivan TD, Cerussi AE, Carpenter PM, Mehta RS, Roblyer D, Yang W, Paulsen KD, Pogue BW, Jiang S, Kaufman PA, Yodh AG, Chung SH, Schnall M, Snyder BS, Hylton N, Boas DA, Carp SA, Isakoff SJ, Mankoff D; ACRIN 6691 investigators.
Predicting Responses to Neoadjuvant Chemotherapy in Breast Cancer: ACRIN 6691 Trial of Diffuse Optical Spectroscopic Imaging.
Cancer Res. 2016 Oct 15;76(20):5933-5944. Epub 2016 Aug 15.
17. Dynamic Diffuse Optical Tomography for Monitoring Neoadjuvant Chemotherapy in Patients with Breast Cancer.
Gunther JE, et al. Radiology. 2018. PMID: 29431574
18. Diffuse optical spectroscopic imaging reveals distinct early breast tumor hemodynamic responses to metronomic and maximum tolerated dose regimens.
Tank A, Peterson HM, Pera V, Tabassum S, Leproux A, O'Sullivan T, Jones E, Cabral H, Ko N, Mehta RS, Tromberg BJ, Roblyer D.
Breast Cancer Res. 2020 Mar 13;22(1):29. doi: 10.1186/s13058-020-01262-1.
19. Zhu Q, Tannenbaum S, Kurtzman SH, DeFusco P, Ricci A Jr, Vavadi H, Zhou F, Xu C, Merkulov A, Hegde P, Kane M, Wang L, Sabbath K
Identifying an early treatment window for predicting breast cancer response to neoadjuvant chemotherapy

using immunohistopathology and hemoglobin parameters.
Breast Cancer Res. 2018 Jun 14;20(1):56. doi: 10.1186/s13058-018-0975-1.

20. Cochran JM, et al. Tissue oxygen saturation predicts response to breast cancer neoadjuvant chemotherapy within 10 days of treatment.
J Biomed Opt. 2018. PMID: 30338678 Free PMC article.
21. Zhu Q, Wang L, Tannenbaum S, Ricci A Jr, DeFusco P, Hegde P.Breast Cancer Res. 2014 Oct 28;16(5):456. doi: 10.1186/s13058-014-0456-0.
Breast cancer: assessing response to neoadjuvant chemotherapy by using US-guided near-infrared tomography.
22. Zhu Q, DeFusco PA, Ricci A Jr, Cronin EB, Hegde PU, Kane M, Tavakoli B, Xu Y, Hart J, Tannenbaum SH.Radiology. 2013 Feb;266(2):433-42. doi: 10.1148/radiol.12112415. Epub 2012 Dec 21.
23. Predicting Treatment Response of Breast Cancer to Neoadjuvant Chemotherapy Using Ultrasound-Guided Diffuse Optical Tomography.
Zhi W, Liu G, Chang C, Miao A, Zhu X, Xie L, Zhou J.
Transl Oncol. 2018 Feb;11(1):56-64. doi: 10.1016/j.tranon.2017.10.011. Epub 2017 Nov 22.
24. Predicting breast tumor response to neoadjuvant chemotherapy with diffuse optical spectroscopic tomography prior to treatment.
Jiang S , Pogue BW, Kaufman PA , Gui J , Jermyn M , Frazee TE , Poplack S, DiFlorio-Alexander R, Wells WA , Paulsen KD
Clin Cancer Res. 2014. 20 (23), 6006-15
25. A Comparison of Near-Infrared Diffuse Optical Imaging and 18F-FDG PET/CT for the Early Prediction of Breast Cancer Response to Neoadjuvant Chemotherapy.
Jiang S, Pogue BW J Nucl Med. 2016. PMID: 27103023
26. Tran WT, Gangeh MJ, Sannachi L, Chin L, Watkins E, Bruni SG, Rastegar RF, Curpen B, Trudeau M, Gandhi S, Yaffe M, Slodkowska E, Childs C, Sadeghi-Naini A, Czarnota GJ
Predicting breast cancer response to neoadjuvant chemotherapy using pretreatment diffuse optical spectroscopic texture analysis.
Br J Cancer. 2017 May 9;116(10):1329-1339. doi: 10.1038/bjc.2017.97. Epub 2017 Apr 18.
27. Vavadi H, Mostafa A, Zhou F, Uddin KMS, Althobaiti M, Xu C, Bansal R, Ademuyiwa F, Poplack S, Zhu Q. Compact ultrasound-guided diffuse optical tomography system for breast cancer imaging. J Biomed Opt. 2018 Oct;24(2):1-9. doi: 10.1117/1.JBO.24.2.021203.
28. Uddin KMS, Mostafa A, Anastasio M, Zhu Q. Two step imaging reconstruction using truncated pseudoinverse as a preliminary estimate in ultrasound guided diffuse optical tomography.
Biomed Opt Express. 2017 Nov 8;8(12):5437-5449. doi: 10.1364/BOE.8.005437.
29. Ogston, KN, Miller ID, Payne S, et al. A new histologic grading system to assess response of breast cancers to primary chemotherapy; prognostic significance and survival. THE BREAST (2003); 12,320-327.
30. Symmans WF , Peintinger F , Hatzis C et al.
Measurement of residual breast cancer burden to predict survival after neoadjuvant chemotherapy.
J Clin Oncol. 2007; 25: 4414-4422

31. Harvey JM, Clark GM, Osborne CK, Allred DC.
Estrogen receptor status by immunohistochemistry is superior to the ligand-binding assay for predicting response to adjuvant endocrine therapy in breast cancer.
J Clin Oncol. 1999 May;17(5):1474-81.
32. Heller G., Seshan V.E., Moskowitz C.S. and Gonen M. (2016) Inference for the difference in the area under the ROC curve derived from nested binary regression models. Biostatistics 18, 260-274.
33. Shin HJ, Kim HH, Ahn JH et al. Comparison of mammography, sonography, MRI and clinical examination in patients with locally advanced or inflammatory breast cancer who underwent neoadjuvant chemotherapy. Br Journ Radiol 2011;84:612-620
34. Li H, Yao L, Jin P et al. MRI and PET/CT for evaluation of the pathological response to neoadjuvant chemotherapy in breast cancer: A systematic review and meta-analysis. The Breast 2018;40:106-115
35. National Comprehensive Cancer Network. Breast Cancer (Version 3.2019).
36. Eisenhauer EA, Therasse B, Bogaerts J et al. New response evaluation criteria in solid tumours: Revised RECIST guideline (version 1.1) Euro Journ of Cancer 2009;45:228-247.
37. Tirkes T, Hollar , Tann M, Kohli , Akisik F, Sandrasegaran K. Response criteria in oncologic imaging: review of traditional and new criteria. Radiographics. 2013 Sep-Oct;33(5):1323-41. doi: 10.1148/rg.335125214.
38. K.R. Levental, H. Yu, L. Kass, J.N. Lakins, M. Egeblad, J.T. Erler, et al., Matrix crosslinking forces tumor progression by enhancing integrin signaling, Cell. 139 (5) (2009) 891–906.
39. D.T. Butcher, T. Alliston, V.M. Weaver, A tense situation: forcing tumour progression, Nat. Rev. Cancer 9 (2) (2009) 108–122.
40. Maier AM, Heil J, Harcos A, Sinn HP, Rauch G, Uhlmann L, Gomez C, Stieber A, Funk A, Barr RG, Hennigs A, Riedel F, Schäfgen B, Hug S, Marmé F, Sohn C, Golatta M.Maier AM, et al. Prediction of pathological complete response in breast cancer patients during neoadjuvant chemotherapy: Is shear wave elastography a useful tool in clinical routine?
Eur J Radiol. 2020 Jul;128:109025. doi: 10.1016/j.ejrad.2020.109025. Epub 2020 May 1.Eur J Radiol. 2020. PMID: 32371182
41. https://bajan.files.wordpress.com/2010/09/principles-of-cancer-chemotherapy.pdf
42. Guerrero-Zotano AL and Arteaga C.L. Neoadjuvant Trials in ER+ Breast Cancer: A Tool for Acceleration of Drug Development and Discovery.
Cancer Discov. 2017, 7(6):561-574.
43. Masuda N, Lee SJ, Ohtani S, Im YH, Lee ES, Yokota I, Kuroi K, Im SA, Park BW, Kim SB, Yanagita Y, Ohno S, Takao S, Aogi K, Iwata H, Jeong J, Kim A, Park KH, Sasano H, Ohashi Y, Toi M. Adjuvant Capecitabine for Breast Cancer after Preoperative Chemotherapy.
N Engl J Med. 2017 Jun 1;376(22):2147-2159. doi: 10.1056/NEJMoa1612645.

Figures

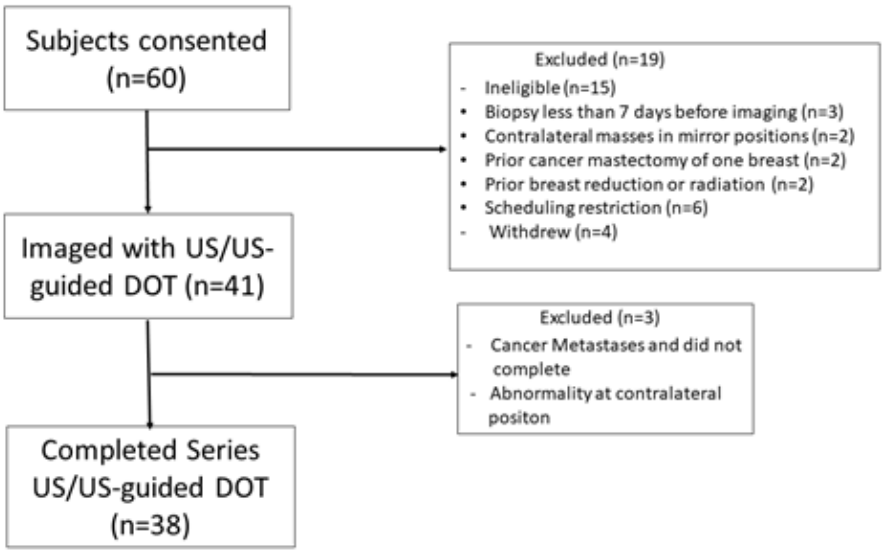

Figure 1

Patient Study Flow Diagram

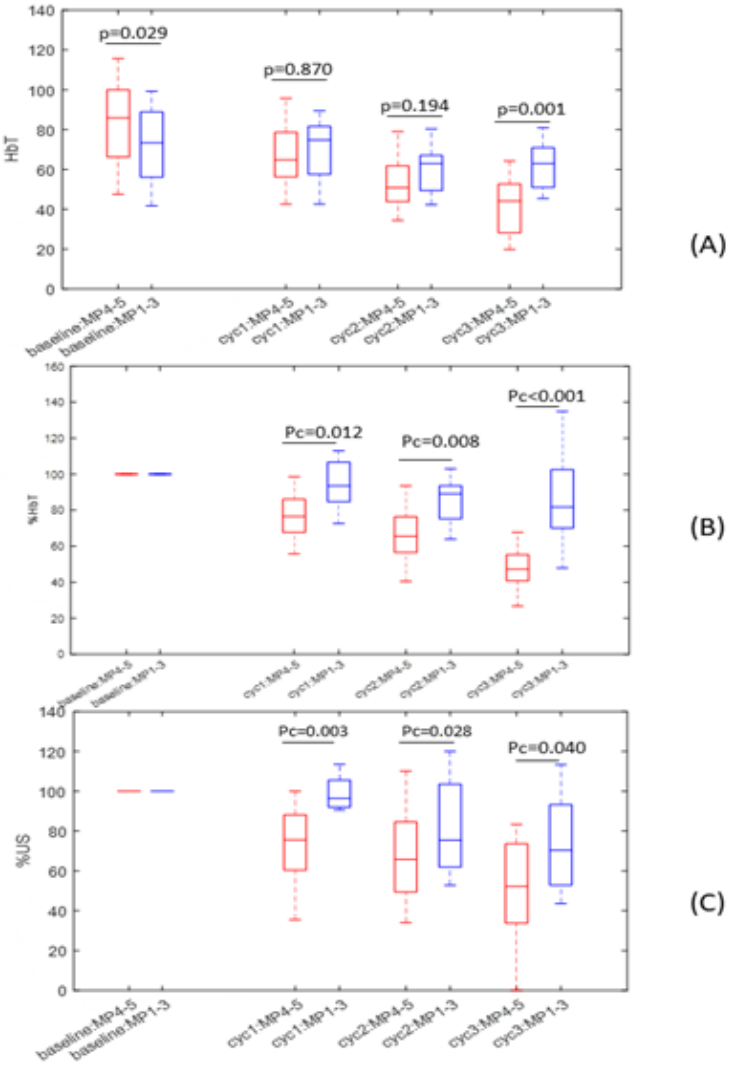

Figure 2

(A) HbT of Miller-Payne grade 4–5 tumors (therapy responders) and grade 1–3 tumors after 1, 2, 3 cycles of neoadjuvant therapy. (B) %HbT of grade 4–5 tumors vs. grade 1–3 tumors after first three cycles of neoadjuvant therapy. (C) %US of grade 4–5 tumors vs. grade 1–3 tumors after first three cycles of neoadjuvant therapy. Pc is Bonferroni-Holm corrected P value.

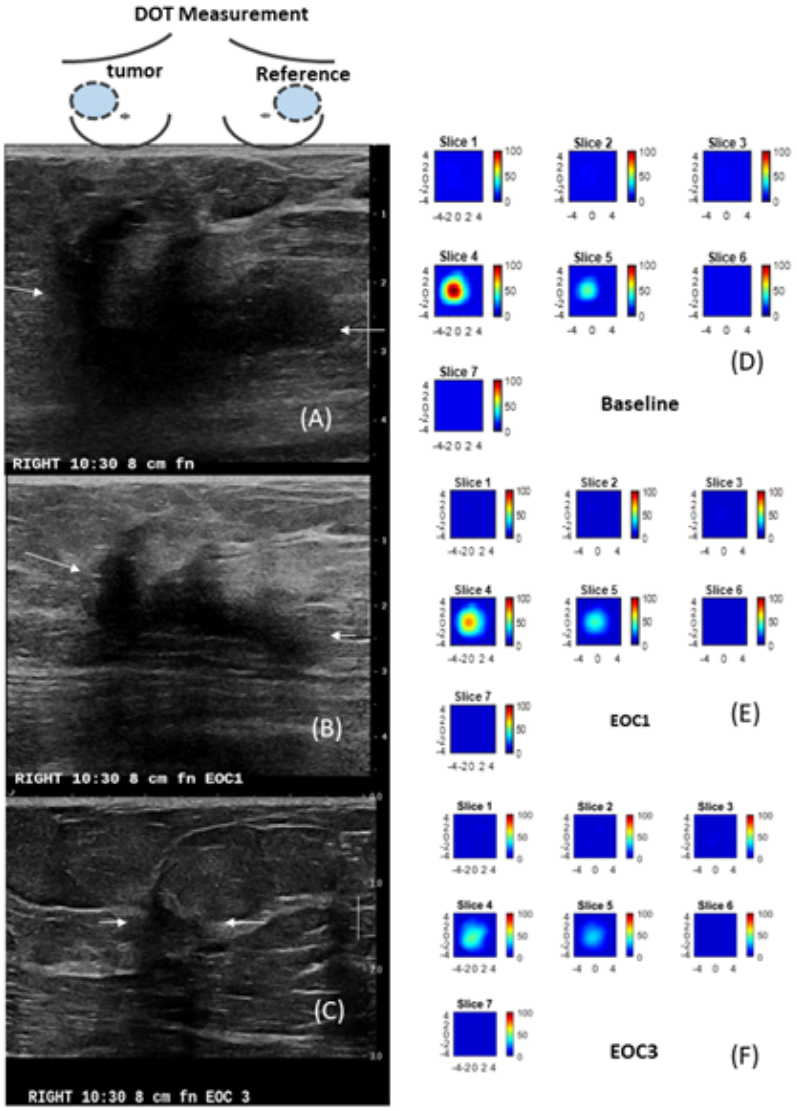

Figure 3

A 59 year-old patient with a T3 triple negative cancer and treated with ACT. The US/DOT imaging were performed at baseline, end of cycle 1 (EOC1), 2, 3, 5 and before surgery. Panel (A)-(C) are co-registered US images obtained at baseline, EOC1 and EOC3. The largest lesion diameters measured by US were 4.6 cm, 3.4 cm,1.0 cm. The corresponding %US at EOC1 and EOC 3 were 73.9% and 21.7%. Panel (E)-(F) are corresponding HbT maps. Each map has 7 slices reconstructed at depths from 0.5 cm to 3.5 cm with 0.5 cm spacing. Each slice has spatial dimensions of 9 cm by 9 cm. The maximum HbT measured at baseline, EOC1, and EOC3 were 108.7 μM, 73.5 μM, and 45.0 μM. The %HbT were 67.6% and 41.4% at EOC1 and EOC3. The patient achieved pCR with Miller-Payne of 5.

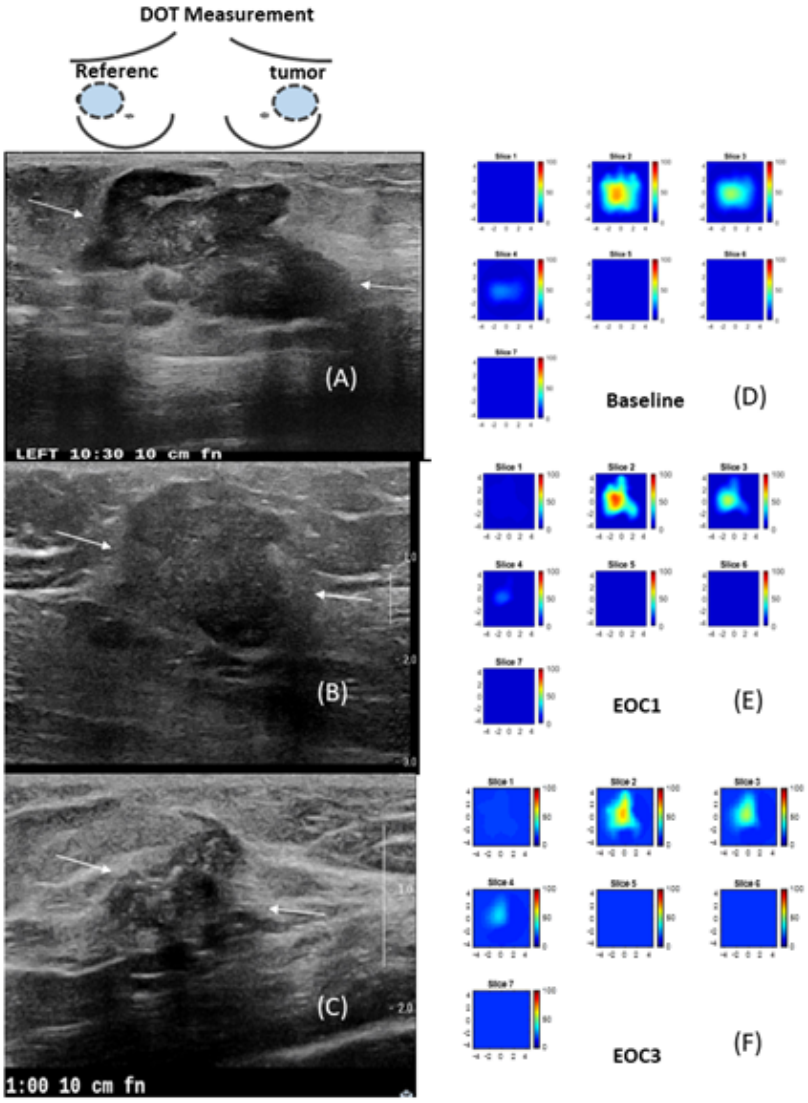

Figure 4

A 62 year-old patient with a T2 ER negative PR positive and HER2 negative IDC and treated with ACT. The US/DOT imaging were performed at baseline, end of cycle 1, 2, 3 and before surgery. Panel (A)-(C) are co-registered US images obtained at baseline, EOC1 and EOC3. The largest lesion diameters measured by US were 3.6 cm, 2.4 cm, 1.7 cm. The corresponding %US at EOC1 and EOC 3 were 66.7% and 47.2%. Panel (E)-(F) are corresponding HbT maps. Each map has 7 slices reconstructed at depths from 0.5 cm to 3.5 cm with 0.5 cm spacing. Each slice has a spatial dimensions of 9 cm by 9 cm. The maximum HbT measured at baseline, EOC1, and EOC3 were 70.3 μM, 79.3μM, and 65.8 μm. The %HbT were 112.8% and 93.6% at EOC1 and EOC3. The patient had 2.4 cm residual tumor with no histologic evidence of tumor response as evaluated after the surgery. Miller-Payne grade was 1.

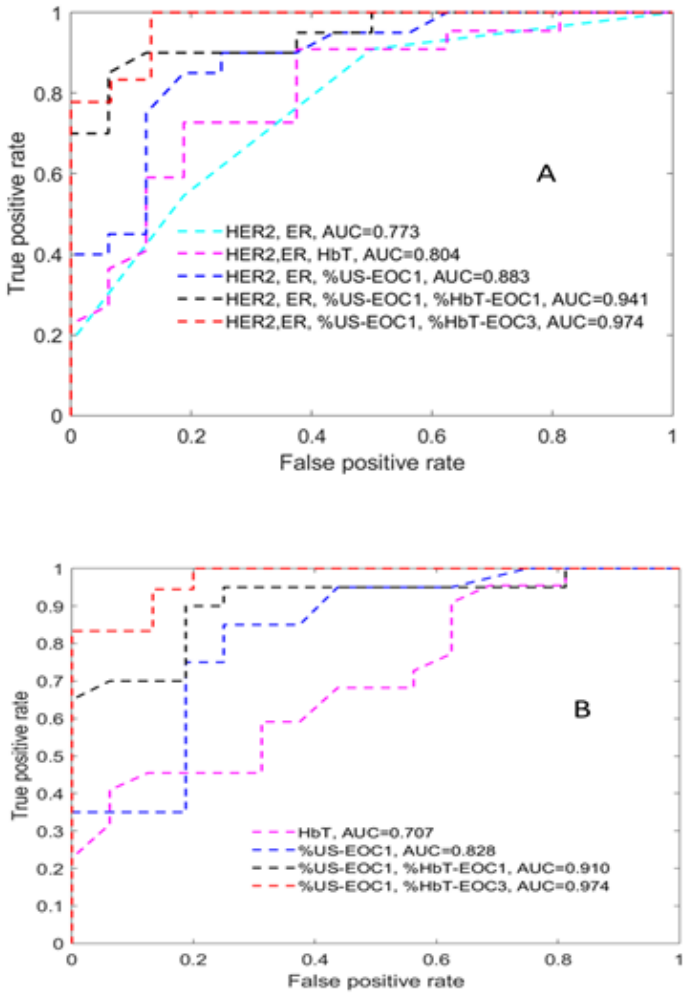

Figure 5

ROCs obtained from different set of predictor variables. (A) ROCs of known HER2/ER subgroup with 5 sets of predictor variables, and (B) ROCs based on HbT, %US-EOC1, %HbT and %US changes regardless of biomarkers.

Supplementary Files

This is a list of supplementary files associated with this preprint. Click to download.

- AppendixA.pdf